Novel monochromatic x-ray generators and their applications to high-speed radiography

Eiichi Sato*[a], Rudolf Germer[b], Haruo Obara[c], Etsuro Tanaka[d], Hidezo Mori[e], Toshiaki Kawai[f], Takashi Inoue[g], Akira Ogawa[g], Mitsuru Izumisawa[h], Toshio Ichimaru[i], Kiyomi Takahashi[j], Shigehiro Sato[j] and Kazuyoshi Takayama[k]

[a]Department of Physics, Iwate Medical University, 3-16-1 Honchodori, Morioka 020-0015, Japan
[b]ITP, FHTW FB1 and TU-Berlin, Blankenhainer Str. 9, D 12249 Berlin, Germany
[c]Department of Radiological Technology, College of Medical Science, Tohoku University, 1-1 Seiryocho, Sendai 980-0872, Japan
[d]Department of Nutritional Science, Faculty of Applied Bio-science, Tokyo University of Agriculture, 1-1-1 Sakuragaoka, Setagaya-ku 156-8502, Japan
[e]Department of Cardiac Physiology, National Cardiovascular Center Research Institute, 5-7-1 Fujishirodai, Suita, Osaka 565-8565, Japan
[f]Electron Tube Division #2, Hamamatsu Photonics Inc., 314-5 Shimokanzo, Iwata 438-0193, Japan
[g]Department of Neurosurgery, School of Medicine, Iwate Medical University, 19-1 Uchimaru, Morioka 020-8505, Japan
[h]Department of Oral Radiology, School of Dentistry, Iwate Medical University, 1-3-27 Chuo, Morioka 020-0021, Japan
[i]Department of Radiological Technology, School of Health Sciences, Hirosaki University, 66-1 Honcho, Hirosaki 036-8564, Japan
[j]Department of Microbiology, School of Medicine, Iwate Medical University, 19-1 Uchimaru, Morioka 020-8505, Japan
[k]Tohoku University Biomedical Engineering Research Organization, 2-1-1 Katahira, Sendai 980-8577, Japan

ABSTRACT

Novel monochromatic x-ray generators and their applications to high-speed radiography are described. The five generators are as follows: a weakly ionized linear plasma x-ray generator, a monochromatic compact flash x-ray generator, a super-fluorescent plasma generator, a cerium x-ray generator using a 3.0-mm-thick aluminum filter, and a 100-μm-focus x-ray generator utilizing the filter. Using the linear plasma generator with a copper target, we observed clean K lines and their harmonics, and soft flash radiography was performed with pulse widths of approximately 500 ns. The compact monochromatic flash x-ray generator produced clean molybdenum K lines easily, and high-speed radiography was performed with pulse widths of approximately 100 ns. Using a steady-state cerium x-ray generator, we performed real-time angiography utilizing an image intensifier and a high-sensitive camera (MLX) made by NAC Image Technology Inc. with a capture time of 1 ms. Finally, real-time magnification radiography was performed by twofold magnification imaging using a 100-μm-focus x-ray generator and the high-sensitive camera.

Keywords: flash radiography, high-speed radiography, high-sped angiography, real-time radiography, enhanced K-edge angiography, high-sensitive CCD camera, image intensifier

1. INTRODUCTION

Conventional flash x-ray generators utilizing high-voltage condensers have been used in high-speed radiography,[1] and single generators have been employed to perform delayed radiography using a trigger delay device. Subsequently, plural flash x-ray generators can be combined to a multi-tube (anode) flash x-ray system to perform extremely high-repetition-rate radiography and multi-direction radiography at desired times. Subsequently, we have developed several different flash x-ray generators[2-5] with photon energies of lower than 150 keV, and these generators have been employed to soft radiography including biomedical applications.

Stroboscopic x-ray generators[6-8] have been developed to primarily perform single and multi-shot radiography using an x-ray film or a computed radiography (CR) system,[9] therefore high-speed real-time radiography can be achieved with a high-speed camera. Although we have developed three stroboscopic generators, major advantages are as follows: maximum repetition rate of approximately 100 kHz, variable x-ray duration, and low noises. Using a special high-voltage pulse generator, the maximum rate can be increased to 1 MHz or beyond.

Recently, we have developed three monochromatic flash x-ray generators[10-18] in order to produce clean K-series characteristic x-rays. The major goal of these developments is to produce slightly coherent clean K lines by x-ray amplification of spontaneous emission of radiation and by increasing the flux of K lines in the plasma. In view of this situation, we have confirmed the irradiation of clean K lines and their harmonics from weakly ionized linear plasmas of nickel and copper.

To perform iodine K-edge angiography using cone beams, we have developed a steady-state cerium x-ray generator[19-21] and have succeeded in observing fine blood vessels and coronary arteries with high contrasts using cerium K lines. Recently, because an extremely high-sensitive CCD camera (MLX) with variable capture times has been developed by NAC Image Technology Inc., stop-motion images can be easily obtained.

Magnification radiography[22] is useful in order to improve the spatial resolution in digital radiography, and narrow –photon-energy bremsstrahlung x-rays with a peak energy of approximately 35 keV from a microfocus tungsten tube are useful for performing high-contrast high-resolution angiography. In magnification radiography, scattering beams from radiographic objects can be reduced without using a grid, and stop-motion images can be taken using the CCD camera.

In this paper, we introduce novel monochromatic x-ray generators, their distinctive radiographic characteristics, and applications to high-speed radiographies including enhanced K-edge angiography.

2. WEAKLY IONIZED LINEAR PLASMA X-RAY GENERATOR

2.1 Generator

Figure 1 shows a block diagram of a high-intensity plasma flash x-ray generator. This generator consists of the following essential components: a high-voltage power supply, a high-voltage condenser with a capacity of approximately 200 nF, a turbomolecular pump, a krytron pulse generator as a trigger device, and a flash x-ray tube. The high-voltage main condenser is charged to 50 kV by the power supply, and electric charges in the condenser are discharged to the tube after triggering the cathode electrode with the trigger device. The plasma flash x-rays are then produced.

The x-ray tube is a demountable cold-cathode triode that is connected to the turbomolecular pump with a pressure of approximately 1 mPa. This tube consists of the following major parts: a hollow cylindrical carbon cathode with a bore diameter of 10.0 mm, a brass focusing electrode, a trigger electrode made from copper wire, a stainless steel vacuum chamber, a nylon insulator, a polyethylene terephthalate (Mylar) x-ray window 0.25 mm in thickness, and a rod-shaped copper target 3.0 mm in diameter with a tip angle of 60°. The distance between the target and cathode electrodes is approximately 20 mm, and the trigger electrode is set in the cathode electrode. As electron beams from the cathode electrode are roughly converged to the target by the focusing electrode, evaporation leads to the formation of a weakly ionized linear plasma, consisting of copper ions and electrons, around the fine target.

In the linear plasma, bremsstrahlung photons with energies higher than the K-absorption edge are effectively absorbed and are converted into fluorescent x-rays. The plasma then transmits the fluorescent rays easily, and bremsstrahlung rays with energies lower than the K-edge are also absorbed by the plasma. In addition, because bremsstrahlung rays are not emitted in the opposite direction to that of electron trajectory, intense characteristic x-rays are generated from the plasma-axial direction.
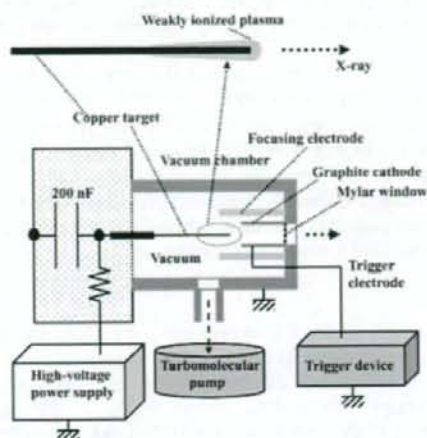
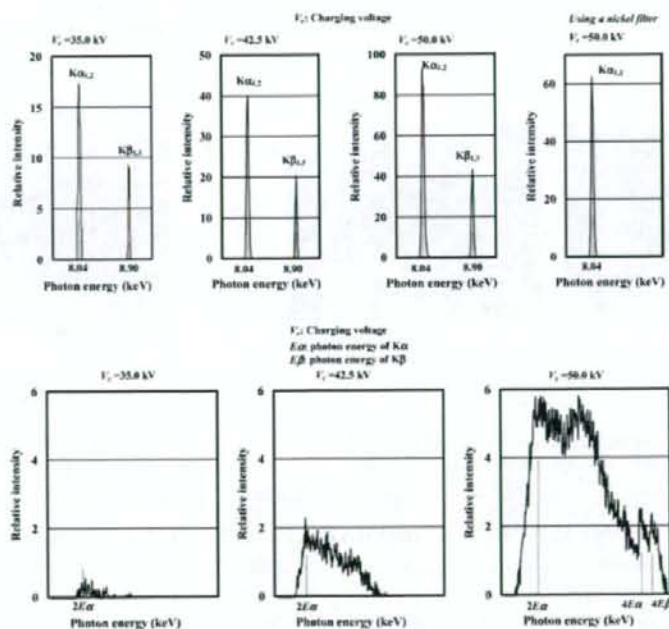Fig. 1. Block diagram of the weakly ionized linear plasma x-ray generator.

Fig. 2. X-ray spectra from weakly ionized linear copper plasma.

2.2 Characteristics

In the flash x-ray generators, the tube voltage and current were measured by a high-voltage divider and a current

transformer, respectively. The tube voltage and current displayed damped oscillations. At a charging voltage of 50 kV, the maximum tube voltage was almost equal to the charging voltage of the main condenser, and the peak current was about 16 kA.

The x-ray pulse widths were approximately 300 ns, and the time-integrated x-ray intensity had a value of approximately 1.5 mGy per pulse at 1.0 m from the x-ray source with a charging voltage of 50 kV.

X-ray spectra from the plasma source were measured by a transmission-type spectrometer with a lithium fluoride curved crystal 0.5 mm in thickness. The spectra were taken by the CR system (Konica Regius 150), and relative x-ray intensity was calculated from Dicom digital data. Figure 2 shows measured spectra from the copper target at the indicated conditions. In fact, we observed clean K lines, and Kα lines were left by absorbing Kβ lines using a 10-μm-thick nickel filter. The characteristic x-ray intensity substantially increased with corresponding increases in the charging voltage, and higher harmonic hard x-rays were observed.

2.3 High-speed radiography

The plasma radiography was performed by the CR system using the filter. The charging voltage and the distance between the x-ray source and imaging plate were 50 kV and 1.2 m, respectively.

First, rough measurements of spatial resolution were made using wires. Radiograms of tungsten wires coiled around pipes made of polymethyl methacrylate (PMMA) are shown in Fig. 3. Although the image contrast decreased somewhat with decreases in the wire diameter, due to blurring of the image caused by the sampling pitch of 87.5 μm, a 50-μm-diameter wire could be observed. Figure 4 shows a radiogram of plastic bullets falling into a polypropylene beaker from a plastic test tube. Because the x-ray duration was about 500 ns, the stop-motion image of bullets could be obtained.
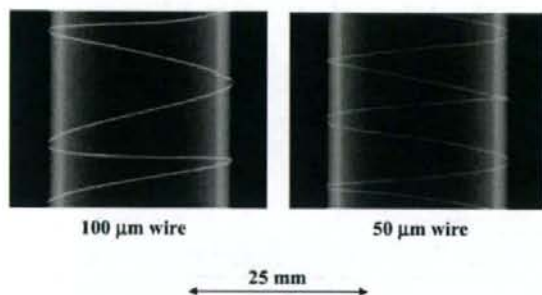

100 μm wire   50 μm wire

25 mm

Fig. 3. Radiograms of tungsten wires coiled around pipes made of polymethyl methacrylate (PMMA).
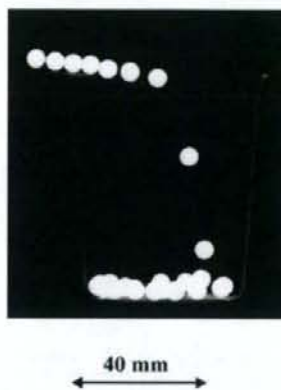

40 mm

Fig. 4. Radiogram of plastic bullets falling into a polypropylene beaker from a plastic test tube.

3. COMPACT MONOCHROMATIC FLASH X-RAY GENERATOR

3.1 Generator

Figure 5 shows a block diagram of a compact monochromatic flash x-ray generator. This generator consists of the following components: a constant high-voltage power supply, a surge Marx generator with a capacity during main discharge of 425 pF, a thyratron trigger device of the surge generator, a turbomolecular pump, and a flash x-ray tube. Since the electric circuit of the high-voltage pulse generator employs a polarity-inversion two-stage Marx line, the surge generator produces twice the potential of the condenser charging voltage. When two condensers inside of the surge generator are charged from −50 to −70 kV, the ideal output voltage ranges from 100 to 140 kV.

The x-ray tube is a demountable diode type, as illustrated in Fig. 6. This tube is connected to the turbomolecular pump with a pressure of about 1 mPa and consists of the following major devices: a rod-shaped molybdenum target 3.0 mm in diameter, a disk cathode made of graphite, a polyethylene terephthalate (Mylar) x-ray window 0.25 mm in thickness, and a polymethyl methacrylate (PMMA) tube body. The target-cathode space was regulated to 1.0 mm from the outside of the x-ray tube by rotating the anode rod, and the transmission x-rays are obtained through a 1.0-mm-thick graphite cathode and an x-ray window. Because bremsstrahlung rays are not emitted in the opposite direction to that of electron trajectory, molybdenum Kα rays can be produced using a 20-μm-thick zirconium K-edge filter.
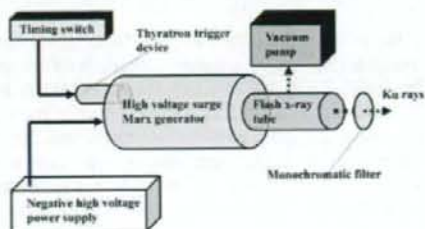

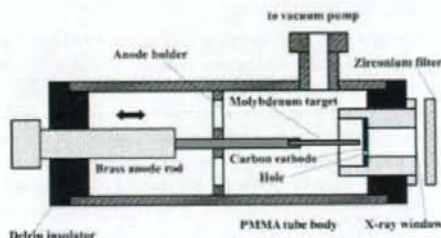Fig. 5. Block diagram of the compact monochromatic flash x-ray generator.

Fig. 6. Structure of the monochromatic flash x-ray tube with a PMMA tube body.

3.2 Characteristics

At a charging voltage of −70 kV, the maximum tube voltage and current were 120 kV and 1.0 kA, respectively. The x-ray pulse widths were approximately 70 ns, and the Kα intensity was approximately 70 μGy per pulse at 0.5 m from the source of 3.0 mm in diameter. In the spectrum measurement, clean molybdenum Kα lines were left using the zirconium filter, and the K-ray intensity substantially increased with increasing the charging voltage (Fig. 7).

3.3 High-speed radiography

The monochromatic flash radiography was performed by the CR system at 0.5 m from the x-ray source with the filter, and the charging voltage was −70 kV. The radiogram of water falling into a polypropylene beaker from a glass test tube is shown in Fig. 8. This image was taken with the slight addition of an iodine-based contrast medium. Because the x-ray duration was about 100 ns, the stop-motion image of water could be obtained.
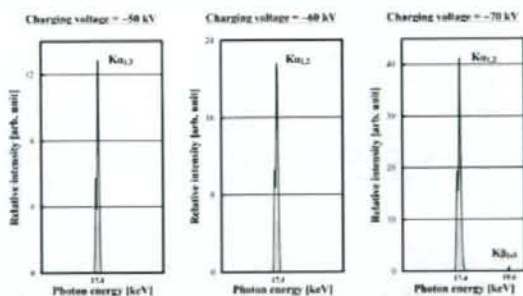

Fig. 7. X-ray spectra from the monochromatic flash x-ray tube with a molybdenum target.

Fig. 8. Radiogram of water falling into a polypropylene beaker from a glass test tube.

4. SUPER-FLUORESCENT PLASMA X-RAY GENERATOR

4.1 Generator

Figure 9 shows a block diagram of a high-intensity super-fluorescent plasma flash x-ray generator. The generator consists of the following essential components: a high-voltage power supply, a high-voltage condenser with a capacity of approximately 150 nF, an air gap switch, a turbomolecular pump, a thyratron pulse generator as a trigger device, and a flash x-ray tube. In this generator, a coaxial cable transmission line is employed in order to increase maximum tube voltage using high-voltage reflection. The high-voltage main condenser is charged up to 80 kV by the power supply, and electric charges in the condenser are discharged to the tube through the four cables after closing the gap switch with the trigger device.

The x-ray tube is a demountable cold-cathode diode that is connected to the turbomolecular pump with a pressure of approximately 1 mPa. This tube consists of the following major parts: a ring-shaped graphite cathode with an inside diameter of 4.5 mm, a stainless-steel vacuum chamber, a nylon insulator, a polyethylene terephthalate (Mylar) x-ray window 0.25 mm in thickness, and a rod-shaped tungsten target 3.0 mm in diameter. The distance between the target and cathode electrodes can be regulated from the outside of the tube, and is set to 1.5 mm. As electron beams from the cathode electrode are roughly converged to the target by the electric field in the tube, evaporation leads to the formation of weakly ionized plasma, consisting of tungsten ions and electrons, at the target tip. Because bremsstrahlung rays are not emitted in the opposite direction to that of electron trajectory, tungsten $K\alpha$ lines are left by absorbing $K\beta$ lines using an ytterbium oxide filter.
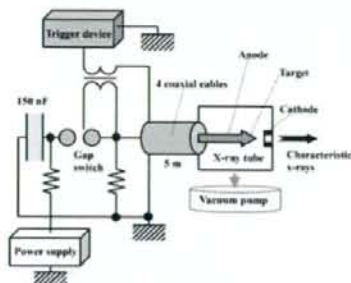

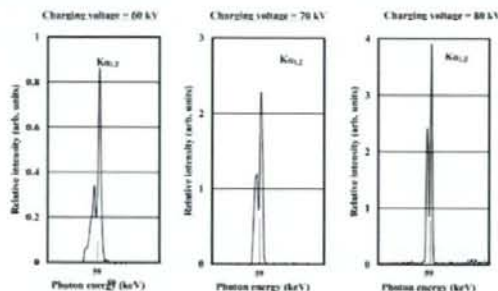Fig. 9. Block diagram of the high-intensity super-fluorescent plasma flash x-ray generator

Fig. 10. X-ray spectra from the super-fluorescent plasma x-ray tube with a tungsten target.

4.2 Characteristics

Since the electric circuit of the high-voltage pulse generator employs a cable transmission line, the high-voltage pulse generator produces twice the potential of the condenser charging voltage. At a charging voltage of 80 kV, the estimated maximum tube voltage and current are approximately 160 kV and 40 kA, respectively. The x-ray pulse widths were approximately 110 ns, and the time-integrated x-ray intensity had a value of approximately 50 µGy at 1.0 m from the x-ray source with a charging voltage of 80 kV using the filter. When the charging voltage was increased using the filter, the characteristic x-ray intensities of tungsten $K\alpha$ lines increased. The $K\alpha$ lines were clean, and hardly any $K\beta$ lines and bremsstrahlung rays were detected (Fig. 10).

4.3 High-speed gadolinium K-edge angiography

Figure 11 shows the mass attenuation coefficients of gadolinium at the selected energies; the coefficient curve is discontinuous at the gadolinium K-edge. The average photon energy of the tungsten $K\alpha$ lines is shown just above the gadolinium K-edge. The average photon energy of tungsten $K\alpha$ lines is 58.9 keV, and gadolinium contrast media with a K-absorption edge of 50.2 keV absorb the lines easily. Therefore, blood vessels were observed with high contrasts.

The flash angiography was performed by the CR system at 1.2 m from the x-ray source, and the charging voltage was 70 kV. Figure 12 shows angiogram of a rabbit head using gadolinium oxide powder, and fine blood vessels of approximately 100 µm were visible.
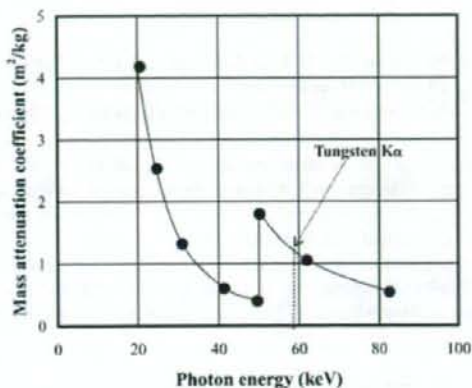
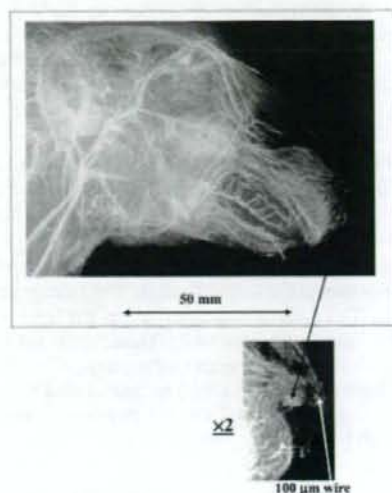Fig. 11. Mass attenuation coefficients of gadolinium and the average photon energy of the tungsten Kα lines.

Fig. 12. Angiogram of a rabbit head using gadolinium oxide powder.

5. CERIUM X-RAY GENERATOR

5.1 Generator

The main circuit for producing x-rays is illustrated in Fig. 13, and employed the Cockcroft-Walton circuit in order to decrease the dimensions of the tube unit. In the x-ray tube, the negative high voltage is applied to the cathode electrode, and the anode (target) is connected to the tube unit case (ground potential) to cool the anode and the target effectively. The filament heating current is supplied by an AC power supply in the controller in conjunction with an insulation transformer. In this experiment, the tube voltage applied was from 45 to 65 kV, and the tube current was regulated to within 0.40 mA (maximum current) by the filament temperature. The exposure time is controlled in order to obtain optimum x-ray intensity. Quasi-monochromatic x-rays are produced using a 3.0-mm-thick aluminum filter for absorbing soft bremsstrahlung rays.
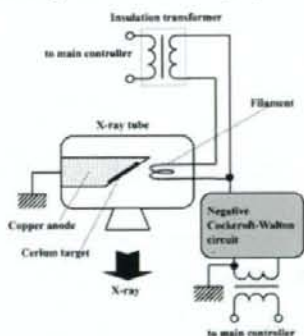

Fig. 13. Main high-voltage transmission line of the cerium x-ray generator.
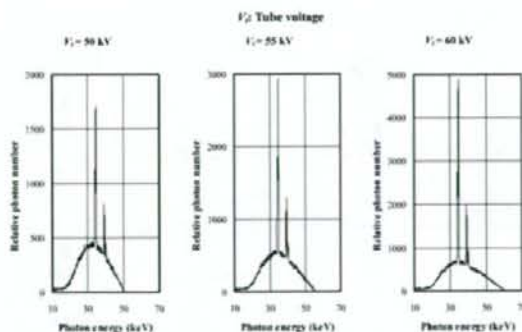

Fig. 14. X-ray spectra using a 3.0-mm-thick aluminum filter with changing the tube voltage.

5.2 Characteristics

The maximum tube voltage and current were 65 kV and 0.4 mA, respectively, and the focal-spot sizes were 1.3×0.9 mm. Cerium K-series characteristic x-rays were left using a 3.0 mm-thick aluminum filter (Fig. 14), and the x-ray intensity was 19.9 μGy/s at 1.0 m from the source with a tube voltage of 60 kV and a current of 0.40 mA.

5.3 High-speed radiography

Real-time cohesion radiography was performed using an image intensifier (I I) and a high-sensitive CCD camera (MLX) made by NAC Image Technology at a frame speed of 30 Hz and an image capture time (shutter speed) of 1 ms (Fig. 15). Radiograms from the I I are taken by the CCD camera, and digital video files are recorded by a personal computer through a video capture box.

Figure 16 shows the mass attenuation coefficients of iodine at the selected energies; the coefficient curve is discontinuous at the iodine K-edge. The average photon energy of the cerium Kα lines is shown just above the iodine K-edge. The average photon energy of Kα lines is 34.6 keV, and iodine contrast media with a K-absorption edge of 33.2 keV absorb the lines easily. Therefore, blood vessels were observed with high contrasts.

Figure 17 shows two frames (angiograms) of water falling into polypropylene beaker from a plastic test tube. These images were taken with a tube voltage of 60 kV, and an iodine-based contrast medium was added a little. Because the capture time was about 1 ms, the stop-motion images of water were obtained. Therefore, blood vessels can be seen with high contrasts.
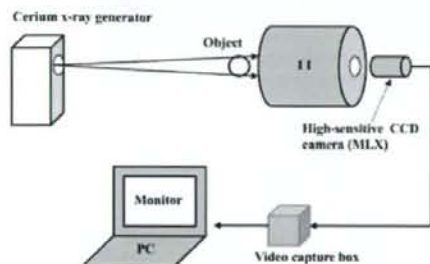

Fig. 15. Experimental setup for performing real-timeradiography with a short capture time utilizing an image intensifier and the MLX camera.
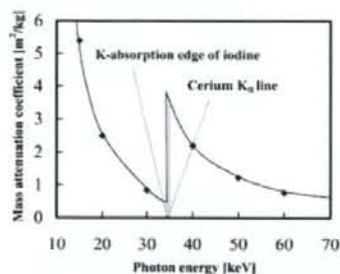

Fig. 16. Mass attenuation coefficients of iodine at the selected energies and the average photon energy of the cerium Kα lines.
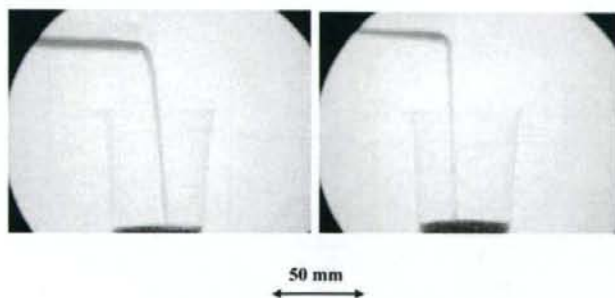

50 mm

Fig. 17. Two angiograms (frames) of water falling into a polypropylene beaker from a plastic test tube using an iodine medium.

6. MICROFOCUS X-RAY GENERATOR

6.1 Generator and experimental setup

The microfocus x-ray generator consists of a main controller, an x-ray tube unit with a Cockcroft-Walton circuit, an insulation transformer, and a 100-μm-focus x-ray tube. The tube voltage, the current, and the exposure time can be controlled by the controller. The main circuit for producing x-rays employs the Cockcroft-Walton circuit in order to decrease the dimensions of the tube unit (Fig. 18). In the x-ray tube, the positive and negative high voltages are applied to the anode and cathode electrodes, respectively. The filament heating current is supplied by an AC power supply in the controller in conjunction with an insulation transformer which is used for isolation from the high voltage from the Cockcroft-Walton circuit. In this experiment, the tube voltage applied was from 45 to 70 kV, and the tube current was regulated to within 0.50 mA (maximum current) by the filament temperature. The exposure time is controlled in order to obtain optimum x-ray intensity, and narrow-photon-energy bremsstrahlung x-rays are produced using a 3.0-mm-thick aluminum filter for absorbing soft x-rays.

6.2 Characteristics

At a constant tube current of 0.50 mA, the x-ray intensity increased when the tube voltage was increased. At a tube voltage of 60 kV, the intensity with the filter was 26.0 μGy/s. Subsequently, in order to measure x-ray spectra, we employed a cadmium telluride detector (XR-100T, Amptek). When the tube voltage was increased, the bremsstrahlung x-ray intensity increased, and both the maximum photon energy and the spectrum peak energy increased.
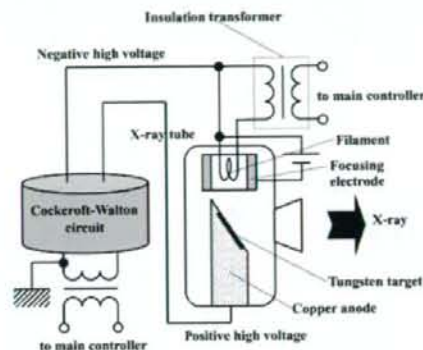
Fig. 18. Circuit diagram of the microfocus x-ray generator.

6.3 High-speed radiography

Real-time magnification radiography was performed by twofold magnification imaging using the I I, the camera, and the filter. The tube voltage, the capture time, and the distance between the x-ray source and the I I were 60 kV, 1 ms, and 1.0 m, respectively. Figure 19 shows radiograms of a metronome, and stop-motion images of a pendulum were observed.

6.4 High-speed enhanced magnification angiography

Figure 20 shows the mass attenuation coefficients of iodine at the selected energies; the coefficient curve is discontinuous at the iodine K-edge. The effective bremsstrahlung x-ray spectra for K-edge angiography are shown above the iodine K-edge. Because iodine contrast media with a K-absorption edge of 33.2 keV absorb the rays easily, blood vessels were observed with high contrasts.

The magnification angiography was performed at the same conditions using iodine microspheres of 15 μm in diameter, and the microspheres (containing 37% iodine by weight) are very useful for making phantoms of non-living animals used for angiography. Angiograms of a dog heart on a turn table is shown in Fig. 21, and the fine coronary arteries are not visible due to the spatial resolution of I I. In addition, neo-capillaries in a rabbit cancer are clearly visible using a high-resolution I I (Fig. 22).
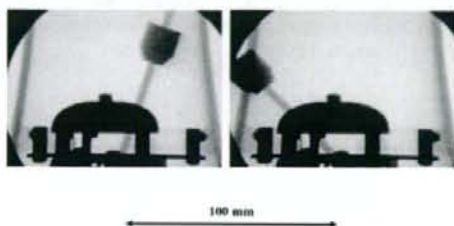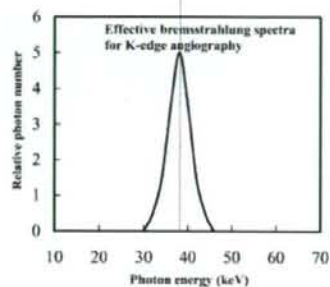
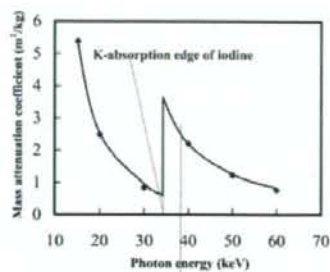Fig. 19. Radiograms of a metronome.

Fig. 20. Mass attenuation coefficients of iodine and effective bremsstrahlung x-rays for enhanced K-edge angiography.
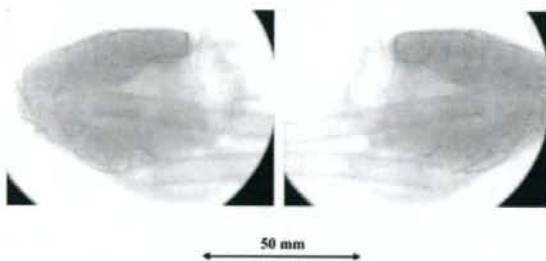

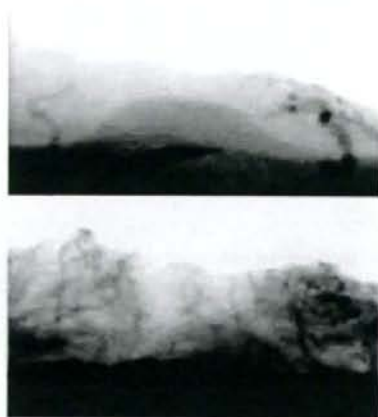Fig. 21. Angiogram of an extracted dog heart using iodine microspheres on a turn table.

Fig. 22. Angiograms of a rabbit cancer using a high-resolution I I.

7. CONCLUSION AND OUTLOOK

We have developed various x-ray generators corresponding to specific radiographic objectives, and the x-ray duration ranges from approximately 100 ns to continuous exposure. In the weakly ionized plasma formation, extremely clean and intense K lines were produced, since the bremsstrahlung x-rays were absorbed effectively by the plasma. In particular, the harmonic bremsstrahlung rays survived and waved due to the x-ray resonation in the plasma.

Although most flash x-ray generators utilize Marx surge generators and produce hard bremsstrahlung x-rays, monochromatic flash x-ray generators have been employed to observe aluminum grains in studies on space debris on the earth. In addition, because the monochromatic tubes realize uniform monochromatic x-ray intensity distributions, the absorber thickness can be calculated easily.

To perform enhanced K-edge angiography using iodine-based contrast media, the cerium, samarium and gadolinium targets are very useful because K lines from these targets are absorbed effectively by iodine media. Therefore, using the x-ray I I in conjunction with the MLX camera with short capture times of approximately 1 ms, stop-motion images of fine blood vessels can be almost seen. Using this image intensifying system, the image quality slightly fell with decreases in the capture time. However, stop-motion image can be obtained when the capture time is decreased.

We employed an x-ray generator with a 100-μm-focus tungsten tube and performed real-time twofold magnification radiography (fluoroscopy) using the I I and the MLX camera. To perform angiography, we employed narrow-photon-energy bremsstrahlung x-rays with a peak photon energy of approximately 35 keV, which can be absorbed easily by iodine-based contrast media. Although we obtained mostly absorption-contrast images, the phase-contrast effect may be added in cases where low-density media are employed.

Because the focus diameter of the tube has been decreased to 10 μm using a rotating anode microfocus tube developed by Hitachi Medical Corporation, a high-resolution and high-speed magnification radiography system will become possible.

ACKNOWLEDGMENTS

REFERENCES

1. R. Germer, "X-ray flash techniques," *J. Phys. E: Sci. Instrum.*, 12, 336-350, 1979.
2. E. Sato, S. Kimura, S. Kawasaki, H. Isobe, K. Takahashi, Y. Tamakawa and T. Yanagisawa, "Repetitive flash x-ray generator utilizing a simple diode with a new type of energy-selective function," *Rev. Sci. Instrum.*, 61, 2343-2348, 1990.
3. A. Shikoda, E. Sato, M. Sagae, T. Oizumi, Y. Tamakawa and T. Yanagisawa, "Repetitive flash x-ray generator having a high-durability diode driven by a two-cable-type line pulser," *Rev. Sci. Instrum.*, 65, 850-856, 1994.
4. E. Sato, K. Takahashi, M. Sagae, S. Kimura, T. Oizumi, Y. Hayasi, Y. Tamakawa and T. Yanagisawa, "Sub-kilohertz flash x-ray generator utilizing a glass-enclosed cold-cathode triode," *Med. & Biol. Eng. & Comput.*, 32, 289-294, 1994.
5. K. Takahashi, E. Sato, M. Sagae, T. Oizumi, Y. Tamakawa and T. Yanagisawa, "Fundamental study on a long-duration flash x-ray generator with a surface-discharge triode," *Jpn. J. Appl. Phys.*, 33, 4146-4151, 1994.
6. E. Sato, Y. Hayasi and Y. Tamakawa, "Recent stroboscopic x-ray generators and their applications to high-speed radiography," *Ann. Rep. Iwate Med. Univ. Lib. Arts and Sci.*, 35, 1-11, 2000.
7. E. Sato, E. Tanaka, H. Mori, T. Kawai, S. Sato, H. Ojima, K. Takayama and H. Ido, "Energy selective high-speed radiography utilizing stroboscopic x-ray generator," *SPIE*, 5580, 765-771, 2005.
8. E. Sato, Y. Hayasi, R. Germer, K. Kimura, E. Tanaka, H. Mori, T. Kawai, T. Inoue, A. Ogawa, S. Sato, K. Takayama and H. Ido, "Energy-selective gadolinium angiography utilizing a stroboscopic x-ray generator," SPIE, 5920, 59200V-1-8, 2005.

9. E. Sato, K. Sato and Y. Tamakawa, "Film-less computed radiography system for high-speed imaging," *Ann. Rep. Iwate Med. Univ. Sch. Lib. Arts and Sci.*, **35**, 13-23, 2000.

10. E. Sato, Y. Hayasi, R. Germer, E. Tanaka, H. Mori, T. Kawai, T. Ichimaru, K. Takayama and H. Ido, "Quasi-monochromatic flash x-ray generator utilizing weakly ionized linear copper plasma," *Rev. Sci. Instrum.*, **74**, 5236-5240, 2003.

11. E. Sato, Y. Hayasi, R. Germer, E. Tanaka, H. Mori, T. Kawai, T. Ichimaru, S. Sato, K. Takayama and H. Ido, "Sharp characteristic x-ray irradiation from weakly ionized linear plasma," *J. Electron Spectrosc. Related Phenom.*, **137-140**, 713-720, 2004.

12. E. Sato, M. Sagae, E. Tanaka, Y. Hayasi, R. Germer, H. Mori, T. Kawai, T. Ichimaru, S. Sato, K. Takayama and H. Ido, "Quasi-monochromatic flash x-ray generator utilizing a disk-cathode molybdenum tube," *Jpn. J. Appl. Phys.*, **43**, 7324-7328, 2004.

13. E. Sato, E. Tanaka, H. Mori, T. Kawai, S. Sato and K. Takayama, "Clean monochromatic x-ray irradiation from weakly ionized linear copper plasma," *Opt. Eng.*, **44**, 049002-1-6, 2005.

14. E. Sato, E. Tanaka, H. Mori, T. Kawai, T. Ichimaru, S. Sato, K. Takayama and H. Ido, "Compact monochromatic flash x-ray generator utilizing a disk-cathode molybdenum tube," *Med. Phys.*, **32**, 49-54, 2005.

15. E. Sato, Y. Hayasi, R. Germer, E. Tanaka, H. Mori, T. Kawai, T. Inoue, A. Ogawa, S. Sato, T. Ichimaru, K. Takayama, J. Onagawa and H. Ido, "Monochromatic flash x-ray generator utilizing a disk-cathode silver tube," *Opt. Eng.*, **44**, 096501-1-6, 2005.

16. E. Sato, Y. Hayasi, K. Kimura, E. Tanaka, H. Mori, T. Kawai, T. Inoue, A. Ogawa, S. Sato, K. Takayama, J. Onagawa and H. Ido, "Enhanced K-edge angiography utilizing tantalum plasma x-ray generator in conjunction with gadolium-based contrast media," *Jpn. J. Appl. Phys.*, **44**, 8716-8721, 2005.

17. E. Sato, Y. Hayasi, R. Germer, K. Kimura, E. Tanaka, H. Mori, T. Kawai, T. Inoue, A. Ogawa, S. Sato, K. Takayama and H. Ido, "Enhanced K-edge plasma angiography achieved with tungsten Kα rays utilizing gadolinium-based contrast media," *SPIE*, **5920**, 592012-1-8, 2005.

18. E. Sato, Y. Hayasi, R. Germer, E. Tanaka, H. Mori, T. Kawai, T. Inoue, A. Ogawa, S. Sato, K. Takayama, J. Onagawa, "X-ray spectra from weakly ionized linear copper plasma," *Jpn. J. Appl. Phys.*, **45**, 5301-5306, 2006.

19. E. Sato, E. Tanaka, H. Mori, T. Kawai, T. Ichimaru, S. Sato, K. Takayama and H. Ido, "Demonstration of enhanced K-edge angiography using a cerium target x-ray generator," *Med. Phys.*, **31**, 3017-3021, 2004.

20. E. Sato, A. Yamadera, E. Tanaka, H. Mori, T. Kawai, F. Ito, T. Inoue, A. Ogawa, S. Sato, K. Takayama, J. Onagawa and H. Ido, "X-ray spectra from a cerium target and their application to cone beam K-edge angiography," *Opt. Eng.*, **44**, 096502-1-6, 2005.

21. E. Sato, E. Tanaka, H. Mori, T. Kawai, T. Inoue, A. Ogawa, A. Yamadera, S. Sato, F. Ito, K. Takayama, J. Onagawa and H. Ido, "Variations in cerium x-ray spectra and enhanced K-edge angiography," *Jpn. J. Appl. Phys.*, **44**, 8204-8209, 2005.

22. E. Sato, E. Tanaka, H. Mori, H. Kawakami, T. Kawai, T. Inoue, A. Ogawa, S. Sato, T. Ichimaru, K. Takayama and H. Ido, "Enhanced magnification angiography including phase-contrast effect using a 100-μm focus x-ray tube," *SPIE*, **5918**, 591811-1-9, 2005.

*dresato@iwate-med.ac.jp; phone +81-19-651-5111; fax +81-19-654-9282

High-sensitive radiography system utilizing a pulse x-ray generator and a night-vision CCD camera (MLX)

Eiichi Sato*[a], Michiaki Sagae[a], Etsuro Tanaka[b], Hidezo Mori[c], Toshiaki Kawai[d], Takashi Inoue[e], Akira Ogawa[e], Shigehiro Sato[f], Toshio Ichimaru[g] and Kazuyoshi Takayama[h]

[a]Department of Physics, Iwate Medical University, 3-16-1 Honchodori, Morioka 020-0015, Japan,
[b]Department of Nutritional Science, Faculty of Applied Bio-science, Tokyo University of Agriculture, 1-1-1 Sakuragaoka, Setagaya-ku 156-8502, Japan
[c]Department of Cardiac Physiology, National Cardiovascular Center Research Institute, 5-7-1 Fujishirodai, Suita, Osaka 565-8565 Japan
[d]Electron Tube Division #2, Hamamatsu Photonics Inc., 314-5 Shimokanzo, Iwata 438-0193, Japan
[e]Department of Neurosurgery, School of Medicine, Iwate Medical University, 19-1 Uchimaru, Morioka 020-8505, Japan
[f]Department of Microbiology, School of Medicine, Iwate Medical University, 19-1 Uchimaru, Morioka 020-8505, Japan
[g]Department of Radiological Technology, School of Health Sciences, Hirosaki University, 66-1 Honcho, Hirosaki 036-8564, Japan
[h]Tohoku University Biomedical Engineering Research Organization, 2-1-1 Katahira, Sendai 980-8577, Japan

ABSTRACT

High-sensitive radiography system utilizing a kilohertz-range stroboscopic x-ray generator and a night-vision CCD camera (MLX) is described. The x-ray generator consists of the following major components: a main controller, a condenser unit with a Cockcroft-Walton circuit, and an x-ray tube unit in conjunction with a grid controller. The main condenser of about 500 nF in the unit is charged up to 100 kV by the circuit, and the electric charges in the condenser are discharged to the triode by the grid control circuit. The maximum tube current and the repetition rate are approximately 0.5 A and 50 kHz, respectively. The x-ray pulse width ranges from 0.01 to 1.0 ms, and the maximum shot number has a value of 32. At a charging voltage of 60 kV and a width of 1.0 ms, the x-ray intensity obtained without filtering was 6.04 µGy at 1.0 m per pulse. In radiography, an object is exposed by the pulse x-ray generator, and a radiogram is taken by an image intensifier. The image is intensified by the CCD camera, and a stop-motion image is stored by a flash memory device using a trigger delay device. The image quality was improved with increases in the x-ray duration, and a single-shot radiography was performed with durations of less than 1.0 ms.

Keywords: high-sensitive radiography, image intensification, high-sensitive CCD camera, pulse x-ray generator

1. INTRODUCTION

With advances in high-voltage pulse technology, high-photon-energy flash x-ray generators[1,2] have been developed utilizing multi-stage Marx generators, and the maximum photon energy has been increased up to approximately 1 MeV for military applications. In contrast, we have developed low-photon-energy flash x-ray generators[3-6] with photon energies of lower than 150 keV, and have performed high-speed soft radiographies including biomedical applications.

To produce extremely clean K-series characteristic x-rays such as lasers, we have developed three characteristic flash x-ray generators[7-15] and have succeeded in producing clean K lines. In particular, bremsstrahlung x-rays are absorbed effectively by weakly ionized metal plasmas. Subsequently, we have developed steady-state characteristic x-ray

generators[16] and have succeeded in producing clean K lines utilizing angle dependence of the bremsstrahlung x-rays.
In the biomedical field, because there are no ultra-high-speed movements, a condenser-discharge stroboscopic x-ray generator[17,18] has been developed. In this generator, the x-ray duration can be controlled from 10 μs to 1.0 ms, and the maximum repetition rate is approximately 50 kHz. In conjunction with a computed radiography (CR) system, short-duration and multi-shot radiographies are possible. In addition, the velocity of a high-speed object can be calculated easily by measuring the length of blurring because the x-ray duration can be controlled correctly within 1.0 ms.

Recently, because an extremely high-sensitive color CCD camera (MLX) has been developed by NAC image technology, we are very interested in intensifying the x-ray image signals using the MLX camera in conjunction with a pulse x-ray generator. Using image intensifying, the absorbed dose can be reduced from patients.

In this research, we employed a stroboscopic x-ray generator and performed a preliminary study on the intensification of image signal, utilizing an image intensifier and the high-sensitive CCD camera.

2. PULSE X-RAY GENERATOR

Figure 1 shows the block diagram of a kilohertz-range stroboscopic x-ray generator. This generator consists of the following major components: a main controller, a condenser unit with a Cockcroft-Walton circuit, and an x-ray tube unit in conjunction with a grid controller. The main condenser of about 500 nF in the unit is charged up to 100 kV by the circuit, and the electric charges in the condenser are discharged to the triode by the grid control circuit. Although the tube voltage decreased during the discharging for generating x-rays, the maximum value was equal to the initial charging voltage of the main condenser.

The x-ray tube is a glass-enclosed hot-cathode triode and is composed of the following major parts: an anode rod made of copper, a tungsten plate target, an iron focusing electrode, a tungsten hot cathode (filament), a tungsten grid, and a glass tube body. The electron beams from the cathode are accelerated between the anode and cathode electrodes and are converged to the target by the focusing electrode. The tube is set in the metal case filled with insulation oil, and the diaphragm regulates the irradiation field.
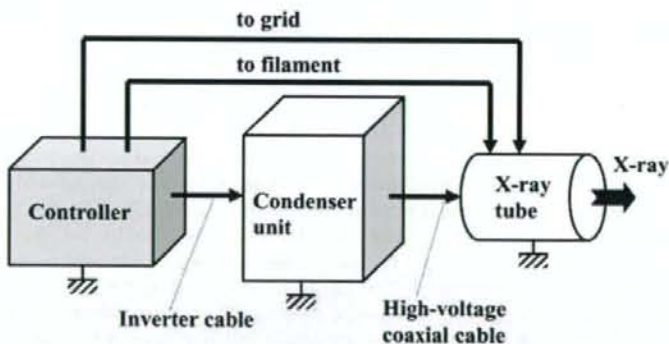

Fig. 1. Block diagram of the kilohertz-range stroboscopic x-ray generator.

3. CHARACTERISTICS

3.1 X-ray output

The x-ray output was detected by a pin diode, and the output voltages from the diode were measured by a digital storage scope (Fig. 2). When the charging voltage was increased, the pulse height increased substantially. Using this generator, the pulse width can be controlled correctly and ranged from 10 μs to 1.0 ms. The maximum repetition rate was approximately 50 kHz, and stable repetitive x-ray pulses were obtained.

3.2 Time-integrated x-ray intensity

Figure 3 shows the time-integrated (absolute) value of the x-ray intensity at 1.0 m per pulse measured by a Victoreen 660 ionization chamber. The intensity was proportional to the x-ray duration. At a constant pulse width of 1.0 ms, the intensity increased with increasing the charging voltage. At a charging voltage of 60 kV and a width of 1.0 ms, the x-ray intensity was 6.04 µGy per pulse at 1.0 m from the source.
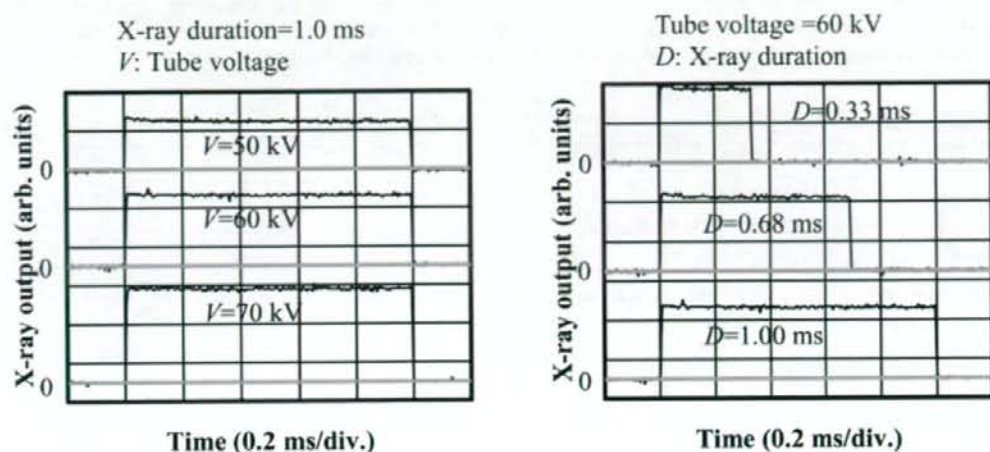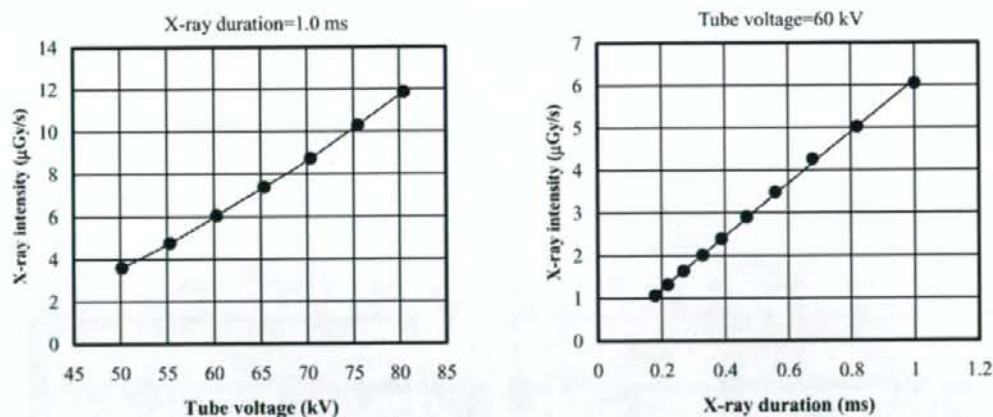

Fig. 2. X-ray outputs at indicated conditions.

Fig. 3. X-ray intensities at 1.0 m from the x-ray source.

4. RADIOGRAPHY

Figure 4 shows the experimental setup for intensifying x-ray image signals using the MLX camera. An object is exposed by the pulse x-ray generator, and a radiogram is taken by an image intensifier. Then, the image is amplified by the CCD camera, and a stop-motion image is stored by a flash memory device using a trigger delay device with a delay time of 50 ms. The image quality improved with increases in the x-ray duration, and single-shot radiography was performed with durations of less than 1.0 ms.

First, rough measurements of spatial resolution were made using wires. Figure 5 shows a radiogram of a 200-μm-diameter tungsten wire coiled around a pipe made of polymethyl methacrylate. In this radiography, the wire was observed with blurring, and image quality improved with increases in the x-ray duration. Next, two radiograms of a metronome are shown in Fig. 6, and stop-motion images of a pendulum are visible. In radiography of plastic bullets, spherical bullets were clearly observed (Fig. 7). Finally, the image of water falling into a polypropylene beaker from a plastic test tube is shown in Fig. 8. This image was taken with the slight addition of an iodine-based contrast medium. Because the x-ray duration was 1 ms, the stop-motion image of water could be obtained.
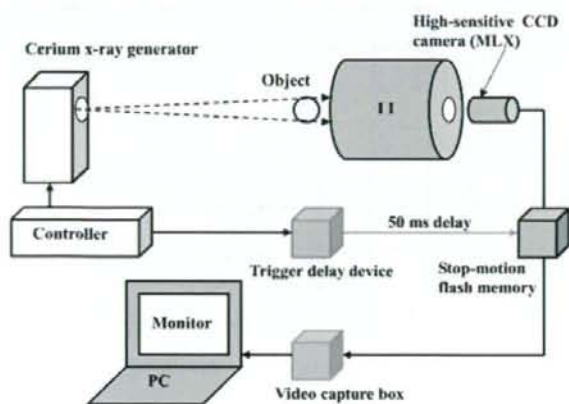

40 mm

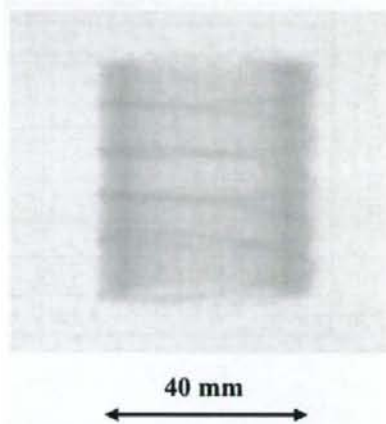Fig. 4. Experimental setup for performing real-time radiography utilizing the MLX camera.

Fig. 5. Radiogram of a 200-μm-diameter tungsten wire coiled around a pipe made of polymethyl methacrylate.
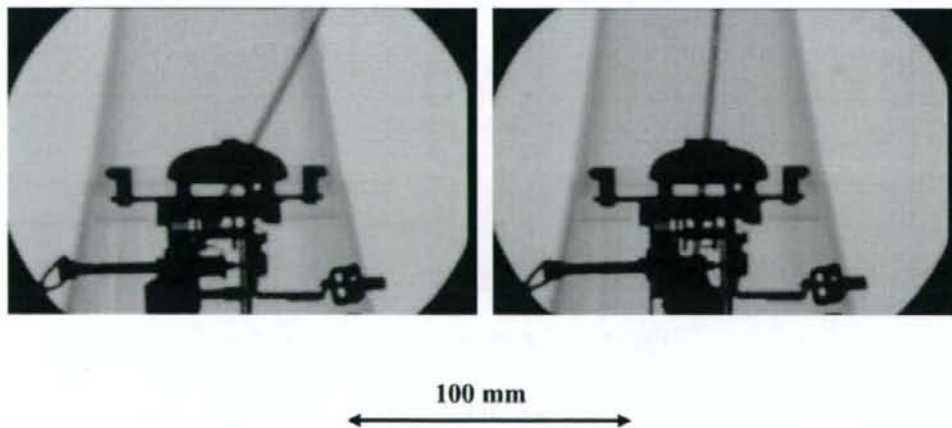

100 mm

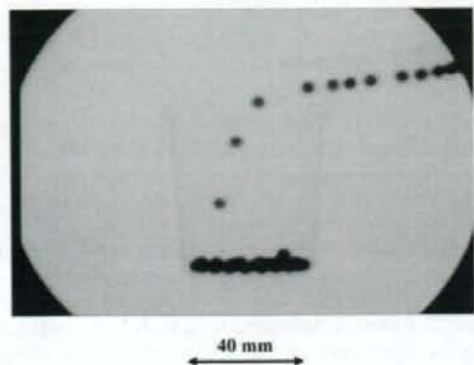Fig. 6. Two radiograms of a metronome.

Fig. 7. Radiogram of plastic bullets falling into a polypropylene beaker from a plastic test tube.
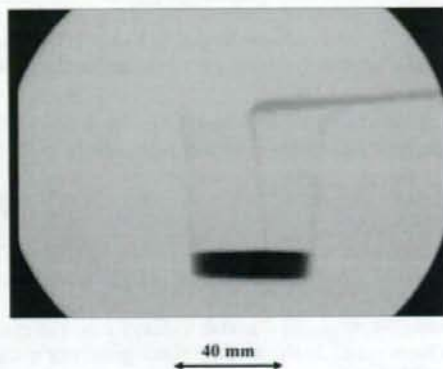
Fig. 8. Radiogram of water falling into a polypropylene beaker from a plastic test tube using an iodine medium.

5. DISCUSSION

We performed a fundamental study on the intensification of the x-ray image signal using the MLX camera, and the image quality improved with increases in the x-ray duration. The spatial resolution was primarily determined by the resolution of I I and the pixel number of the camera. Therefore, the resolution improves with improving the I I resolution and with increasing the pixel number.

Without considering the absorbed dose, short-duration real-time radiography is possible by decreasing the image capture time of the camera using a steady-state x-ray generator. In cases where a microfocus x-ray generator is employed, the spatial resolution improves using magnification radiography, and the real-time radiography with a capture time of 1 ms can be performed by image intensifying.

In this experiment, although we performed only single-shot radiography, high-speed dynamic radiography could be possible using a high-speed high-sensitive video camera synchronizing to the repetitive x-ray output, and the repetition rate can be increased to approximately 50 kHz.

ACKNOWLEDGMENTS

REFERENCES

1. A. Mattsson, "Some characteristics of a 600 kV flash x-ray tube," *Physica Scripta*, **5**, 99-102, 1972.
2. R. Germer, "X-ray flash techniques," *J. Phys. E: Sci. Instrum.*, **12**, 336-350, 1979.
3. E. Sato, S. Kimura, S. Kawasaki, H. Isobe, K. Takahashi, Y. Tamakawa and T. Yanagisawa, "Repetitive flash x-ray generator utilizing a simple diode with a new type of energy-selective function," *Rev. Sci. Instrum.*, **61**, 2343-2348, 1990.

4. A. Shikoda, E. Sato, M. Sagae, T. Oizumi, Y. Tamakawa and T. Yanagisawa, "Repetitive flash x-ray generator having a high-durability diode driven by a two-cable-type line pulser," *Rev. Sci. Instrum.*, **65**, 850-856, 1994.

5. E. Sato, K. Takahashi, M. Sagae, S. Kimura, T. Oizumi, Y. Hayasi, Y. Tamakawa and T. Yanagisawa, "Sub-kilohertz flash x-ray generator utilizing a glass-enclosed cold-cathode triode," *Med. & Biol. Eng. & Comput.*, **32**, 289-294, 1994.

6. K. Takahashi, E. Sato, M. Sagae, T. Oizumi, Y. Tamakawa and T. Yanagisawa, "Fundamental study on a long-duration flash x-ray generator with a surface-discharge triode," *Jpn. J. Appl. Phys.*, **33**, 4146-4151, 1994.

7. E. Sato, Y. Hayasi, R. Germer, E. Tanaka, H. Mori, T. Kawai, T. Ichimaru, K. Takayama and H. Ido, "Quasi-monochromatic flash x-ray generator utilizing weakly ionized linear copper plasma," *Rev. Sci. Instrum.*, **74**, 5236-5240, 2003.

8. E. Sato, Y. Hayasi, R. Germer, E. Tanaka, H. Mori, T. Kawai, T. Ichimaru, S. Sato, K. Takayama and H. Ido, "Sharp characteristic x-ray irradiation from weakly ionized linear plasma," *J. Electron Spectrosc. Related Phenom.*, **137-140**, 713-720, 2004.

9. E. Sato, M. Sagae, E. Tanaka, Y. Hayasi, R. Germer, H. Mori, T. Kawai, T. Ichimaru, S. Sato, K. Takayama and H. Ido, "Quasi-monochromatic flash x-ray generator utilizing a disk-cathode molybdenum tube," *Jpn. J. Appl. Phys.*, **43**, 7324-7328, 2004.

10. E. Sato, E. Tanaka, H. Mori, T. Kawai, S. Sato and K. Takayama, "Clean monochromatic x-ray irradiation from weakly ionized linear copper plasma," *Opt. Eng.*, **44**, 049002-1-6, 2005.

11. E. Sato, E. Tanaka, H. Mori, T. Kawai, T. Ichimaru, S. Sato, K. Takayama and H. Ido, "Compact monochromatic flash x-ray generator utilizing a disk-cathode molybdenum tube," *Med. Phys.*, **32**, 49-54, 2005.

12. E. Sato, Y. Hayasi, R. Germer, E. Tanaka, H. Mori, T. Kawai, T. Inoue, A. Ogawa, S. Sato, T. Ichimaru, K. Takayama, J. Onagawa and H. Ido, "Monochromatic flash x-ray generator utilizing a disk-cathode silver tube," *Opt. Eng.*, **44**, 096501-1-6, 2005.

13. E. Sato, Y. Hayasi, K. Kimura, E. Tanaka, H. Mori, T. Kawai, T. Inoue, A. Ogawa, S. Sato, K. Takayama, J. Onagawa and H. Ido, "Enhanced K-edge angiography utilizing tantalum plasma x-ray generator in conjunction with gadolium-based contrast media," *Jpn. J. Appl. Phys.*, **44**, 8716-8721, 2005.

14. E. Sato, Y. Hayasi, R. Germer, K. Kimura, E. Tanaka, H. Mori, T. Kawai, T. Inoue, A. Ogawa, S. Sato, K. Takayama and H. Ido, "Enhanced K-edge plasma angiography achieved with tungsten Kα rays utilizing gadolinium-based contrast media," *SPIE*, **5920**, 592012-1-8, 2005.

15. E. Sato, Y. Hayasi, R. Germer, E. Tanaka, H. Mori, T. Kawai, T. Inoue, A. Ogawa, S. Sato, K. Takayama, J. Onagawa, "X-ray spectra from weakly ionized linear copper plasma," *Jpn. J. Appl. Phys.*, **45**, 5301-5306, 2006.

16. E. Sato, E. Tanaka, H. Mori, T. Kawai, T. Inoue, A. Ogawa, S. Sato, K. Takayama and J. Onagawa, "Characteristic x-ray generator utilizing angle dependence of bremsstrahlung x-ray distribution," *Jpn. J. Appl. Phys.*, **45**, 2845-2849, 2006.

17. E. Sato, E. Tanaka, H. Mori, T. Kawai, S. Sato, H. Ojima, K. Takayama and H. Ido, "Energy selective high-speed radiography utilizing stroboscopic x-ray generator," *SPIE*, **5580**, 765-771, 2005.

18. E. Sato, Y. Hayasi, R. Germer, K. Kimura, E. Tanaka, H. Mori, T. Kawai, T. Inoue, A. Ogawa, S. Sato, K. Takayama and H. Ido, "Energy-selective gadolinium angiography utilizing a stroboscopic x-ray generator," SPIE, **5920**, 59200V-1-8, 2005.

*dresato@iwate-med.ac.jp; phone +81-19-651-5111; fax +81-19-654-9282

Full Paper

Edaravone Preserves Coronary Microvascular Endothelial Function After Ischemia/Reperfusion on the Beating Canine Heart In Vivo

Renan Sukmawan[1,*], Toyotaka Yada[2], Eiji Toyota[1], Yoji Neishi[1], Teruyoshi Kume[1], Yoshiro Shinozaki[3], Hidezo Mori[4], Yasuo Ogasawara[2], Fumihiko Kajiya[2], and Kiyoshi Yoshida[1]

Departments of [1]Cardiology and [2]Medical Engineering and Systems Cardiology, Kawasaki Medical School, Kurashiki 701-0192, Japan
[3]Department of Physiology, Tokai University School of Medicine, Isehara 259-1193, Japan
[4]Department of Cardiac Physiology, National Cardiovascular Center Research Institute, Suita 565-8565, Japan

Abstract. We examined whether edaravone (3-methyl-1-phenyl-2-pyrazolin-5-one), a free radical scavenger, exerts its protective effect on coronary microvessels after ischemia/reperfusion (I/R) in vivo. Ninety-minute coronary occlusion followed by reperfusion was performed in 16 open-chest dogs with and without edaravone administration. Coronary small artery ($\geq 100\,\mu$m in size) and arteriolar ($<100\,\mu$m) vasodilation, in the presence of endothelium-dependent (acetylcholine) or -independent (papaverine) vasodilators, was directly observed using intravital microscopy before and after I/R. I/R impaired microvascular vasodilation in response to acetylcholine, whereas administration of edaravone preserved the response in microvessels of both sizes, but to a greater extent in the coronary small arteries. No significant changes were noted with papaverine administration. In the edaravone group, the fluorescent intensity from reactive oxygen species (ROS) was lower, whereas nitric oxide (NO) intensity was higher relative to controls in the microvessels of the ischemic area. In conclusion, edaravone preserves coronary microvascular endothelial function after I/R in vivo. These effects, which were NO-mediated, were attributed to the ROS scavenging properties of edaravone.

Keywords: coronary microvessel, edaravone, ischemia/reperfusion, reactive oxygen species, nitric oxide (NO)

Introduction

Coronary microvessels play a pivotal role in the regulation of coronary blood flow (1, 2). Dysfunction of coronary microvessels, especially the resistance vessels, has been associated with an increase in future cardiovascular events in patients with coronary diseases (3, 4). Even in normal subjects, coronary microvascular dysfunction has been shown to increase the risk for a cerebrovascular event (5).

Ischemia/reperfusion (I/R) may result in microvascular dysfunction that further attenuates cardiac func-

tional recovery (6 – 8). One of the central mechanisms responsible for the adverse effect of I/R is free radical production, which includes reactive oxygen species (ROS) (9, 10). A burst of ROS is generated during ischemia and in early reperfusion. This burst overwhelms the antioxidant defense band and causes disturbance in the cardiovascular system (11, 12).

Edaravone (3-methyl-1-phenyl-2-pyrazolin-5-one), a potent free radical scavenger, has been shown to protect cardiomyocytes and brain against I/R injury (13, 14). However, the beneficial effects on coronary microcirculation after I/R remains unknown. We sought to define the effects of edaravone on coronary microvessels after I/R in vivo by 1) direct observation of endothelium-dependent and -independent vasodilation of subepicardial coronary microvessels on the beating canine heart using a charged couple device (CCD) intravital microscope and 2) In-situ detection of ROS and

nitric oxide (NO) in coronary microvessels.

Material and Methods

Animal preparation

We conformed to the Guideline on Animal Experiments and the Guide for the Care and Use of Laboratory Animals published by the National Institutes of Health (NIH) of the United States and the Guiding Principles for the Care and Use of Laboratory Animals approved by the Japanese Pharmacological Society. Sixteen adult mongrel dogs of either sex (15 – 24 kg; purchased from Nagoyalab Service, Mizunami) were premedicated with ketamine (10 mg/kg, i.m.) and anesthetized with sodium pentobarbital (25 mg/kg, i.v.). Each animal was intubated and mechanically ventilated (model VS-600; Instrumental Development, Pittsburgh, PA, USA) with 2% – 3% fluorethane. Blood gas and oxygen saturation were controlled within physiologic ranges throughout the experiment. Open-chest surgery was performed by medial sternotomy and the left anterior descending artery (LAD) was isolated free from surrounding tissue at proximal and medial portions. A transonic flow probe (T206; Transonic Systems, Ithaca, NY, USA) was placed at the medial portion of the LAD to measure the coronary flow rate. A clamp was placed at the proximal LAD to produce coronary occlusion and reperfusion. Visible native collateral vessels were ligated to limit collateral flow into the ischemic area during LAD occlusion. A 6F-catheter was inserted into the right carotid artery through the left coronary artery to administer the vasodilator.

Experimental protocols

After instrumentation, a minimum of 30 min were allowed for stabilization while monitoring hemo-dynamic variables. The study protocol was as follows: i) The arteriolar vasodilatory response to endothelium-dependent (acetylcholine, 1 μg/kg, i.c.; Daiichi Pharma-ceutical Co., Ltd., Tokyo) and -independent (papaverine, 1 mg, i.c.; Dainippon Sumitomo Pharma Co., Ltd., Osaka) vasodilators were examined before and after coronary I (90 min)/R (60 min) under the following conditions: a) control condition, and b) edaravone administration (3 mg/kg, i.v.; supplied by Mitsubishi Pharma Co., Ltd., Osaka) before coronary occlusion. Microspheres were administered at 85 min of coronary occlusion to measure regional myocardial blood flow (MBF). ii) Fluorescent treatment to assess microvascular ROS and NO were performed in 6 dogs (n = 3, each group) after a 60-min reperfusion period. iii) In another 10 dogs (n = 5, each), reperfusion was continued for 5 h and the infarct size and regional MBF were measured.

Intravital CCD microscopy

Direct observation of coronary microvascular vaso-dilation on the beating heart was performed by using a needle-probe intravital CCD microscope (VMS 1210; Nihon Kohden, Tokyo). It contains a gradient index lens (with a magnification of 200) surrounded by light guide fibers and a double lumen sheath. To avoid direct compression of the vessels by the needle-tip, a doughnut-shaped balloon had been installed (15). Vascular images were acquired by gently placing the needle-probe on subepicardial microvessels and were recorded at 30 frames/s. Off-line quantitative analysis was performed using an NIH image analysis software by measuring maximum diameter changes during acetylcholine or papaverine administration.

In situ detection of ROS and NO in coronary micro-vessels

After reperfusion, the heart was immediately removed. The LAD orifice and left circumflex (LCX) artery were cannulated for a continuous phosphate-buffered saline (PBS) infusion. Small tissue blocks were taken from both ischemic (LAD area) and non-ischemic regions (LCX area), and they were frozen in optimal cutting temperature compound (Tissue-Tek; Sakura Fine Chemical, Tokyo) within a few hours. Fluorescent images of the microvessels were obtained using a fluorescent microscope (Olympus BX 51; Olympus, Tokyo). Dihydroethidium (DHE; Molecular Probes, Eugene, OR, USA) and 4,5-diaminofluorescein diacetate (DAF-2DA; Daiichi Pure Chemicals, Tokyo) were used to detect ROS and NO production, respec-tively (16). Five regions of interest (ROI) were selected within the intimal layer of each microvessel. Fluorescent intensities of ROS and NO in the microvessels were measured by NIH software. The average value of the peak fluorescent intensity from each ROI was divided by background intensity (relative intensity) and noted as the microvascular ROS or NO intensities.

Western blotting

Myocardial tissue samples from the LAD and LCX area in each group were isolated for western blotting to assess endogenous NO synthase (eNOS) protein expres-sion after I/R, as previously described (8, 16). Briefly, myocardial tissues were homogenized in the lysis buffer. After centrifugation, the supernatant was collected for immunoblotting. The proteins were transferred by semi-dry electroblotting to polyvinylidene difluoride mem-branes. The blots were then blocked and incubated with rabbit anti-eNOS polyclonal antibody (0.1 μg/ml; Santa Cruz Biotechnology, Santa Cruz, CA, USA) or anti-actin antibody (Santa Cruz Biotechnology) for 120 min